MOLECULAR PAIN

RESEARCH   **Open Access**

Effect of amitriptyline on tetrodotoxin-resistant Na$_v$1.9 currents in nociceptive trigeminal neurons

Jingyao Liang[1†], Xiaoyan Liu[2†], Jianquan Zheng[2] and Shengyuan Yu[1*]

Abstract

Background: Amitriptyline (AMI) is tricyclic antidepressant that has been widely used to manage various chronic pains such as migraines. Its efficacy is attributed to its blockade of voltage-gated sodium channels (VGSCs). However, the effects of AMI on the tetrodotoxin-resistant (TTX-r) sodium channel Na$_v$1.9 currents have been unclear to present.

Results: Using a whole-cell patch clamp technique, this study showed that AMI efficiently inhibited Na$_v$1.9 currents in a concentration-dependent manner and had an IC$_{50}$ of 15.16 μM in acute isolated trigeminal ganglion (TG) neurons of the rats. 10 μM AMI significantly shifted the steady-state inactivation of Na$_v$1.9 channels in the hyperpolarizing direction without affecting voltage-dependent activation. Surprisingly, neither 10 nor 50 μM AMI caused a use-dependent blockade of Na$_v$1.9 currents elicited by 60 pulses at 1 Hz.

Conclusion: These data suggest that AMI is a state-selective blocker of Na$_v$1.9 channels in rat nociceptive trigeminal neurons, which likely contributes to the efficacy of AMI in treating various pains, including migraines.

Keywords: Amitriptyline, Na$_v$1.9, Patch clamp, Trigeminal ganglion, Pain

Background

Amitriptyline (AMI) is a tricyclic antidepressant that has also been widely used to treat different types of chronic pain, such as migraines and diabetic neuropathic pain [1,2]. The antidepressant action is known to inhibit the presynaptic reuptake of norepinephrine and/or serotonin and thus increase concentrations of these neurotransmitters at the synaptic cleft [3,4]. However, its analgesic efficacy is poorly correlated with its antidepressant action because antidepressants are analgesic in patients with chronic pain and no concomitant depression [5] and selective serotonin reuptake inhibitors (SSRIs) are typically ineffective in treating neuropathic pain [6]. Although the mechanism underlying AMI analgesic action is not fully understood, AMI inhibits voltage-gated sodium channels (VGSCs) to reduce the generation and conduction of action potentials in sensory neurons, even more than the local anesthetic bupivacaine, which could in partly explain its efficacy in relieving pain [7-9].

VGSCs Na$_v$1.1-Na$_v$1.9 play critical roles in electrical signaling through action potential generation and propagation in the nervous system; some specific channel subtypes have been implicated in a number of chronic pain conditions. According to their relative sensitivity to tetrodotoxin (TTX), VGSCs are classified as TTX-sensitive (TTX-s) channels (Na$_v$1.1-Na$_v$1.4, Na$_v$1.6 and Na$_v$1.7) and TTX-resistant (TTX-r) channels (Na$_v$1.5, Na$_v$1.8 and Na$_v$1.9)[10]. Na$^+$ currents blocked by AMI were first found in studies of AMI toxicity in the heart, which was supported by a study in which AMI potently inhibited recombinat cardiac hNa$_v$1.5 currents [11]. AMI almost completely inhibited veratridine- or scorpion toxin-evoked efflux of endogenous dopamine (DA) and gamma-aminobutyric acid (GABA) from rat striatal slices by its blockade of Na$^+$ influxes and significantly blocked Na$^+$ currents in a use-dependent manner in cultured GH3 cells [12]. In bovine adrenal chromaffin cells, AMI blocked Na$^+$ currents and caused a hyperpolarizing shift of the steady-state inactivation curve [13]. In cultured rat cortical neurons, AMI not only altered the activation and steady-state inactivation curves of TTX-s Na$^+$ currents toward hyperpolarization but also decreased mRNA expression of Na$_v$1.1, Na$_v$1.2 and

* Correspondence: yushengyuan301@yahoo.com
†Equal contributors
[1]Department of Neurology, Chinese PLA General Hospital, Beijing 100853, PR China
Full list of author information is available at the end of the article

$Na_v1.6$ channels [14]. In addition, both TTX-s and TTX-r Na^+ currents were reduced by AMI in a dose- and holding potential-dependent manner in rat dorsal root ganglion (DRG) neurons [15]. Moreover, regardless of the heterologous expression of $Na_v1.8$ in ND7/23 cells or $hNa_v1.7$ in HEK293 cells, Na^+ currents were effectively inhibited by AMI in concentration-, use- and state-dependent manners [16]. Collectively, these findings provided evidence that AMI could block a variety of VGSC currents in different manners in different cells.

To our knowledge, the effects of AMI on $Na_v1.9$ currents in any cell types have not been reported, although AMI has been shown to dramatically block TTX-r Na^+ channels in rat trigeminal ganglion (TG) neurons [17] as well as in rat DRG neurons [15]. There are at least two subtypes of TTX-r Na^+ channels, i.e., $Na_v1.8$ and $Na_v1.9$, which differ in many respects, such as channel activation/inactivation kinetics and pharmacological properties. $Na_v1.8$ channels are activated at relatively depolarized potentials (around −40 mV) and inactivated more slowly than TTX-s Na^+ channels [18,19], similar to the classic TTX-r Na^+ channels [20]. $Na_v1.9$ channel activation occurs at hyperpolarized potentials (around −70 mV, close to the resting membrane potential), and its inactivation is ultraslow compared to $Na_v1.8$ and TTX-s Na^+ channels [21]. As a result, $Na_v1.9$ channel activation and inactivation are widely overlapping around the resting potential, leading to the production of a persistent current [22,23]. $Na_v1.8$ channels contribute to the majority of the depolarizing inward current of action potentials in neurons in which it is expressed [24,25], whereas $Na_v1.9$ channels modulate resting membrane potential and responses to subthreshold stimuli and to depolarization, which could in turn amplify depolarizing inputs and increase excitability of nociceptive sensory neurons [26]. Both channels are remarkably specifically expressed in small-diameter TG and DRG neurons with thinly myelinated (Aδ) or unmyelinated axons and are likely to be implicated in the molecular mechanisms of nociception and pain [27-30].

Recently, we found that the systemic administration of AMI significantly alleviated nociceptive pains induced by electrical stimulation of the dura mater surrounding the superior sagittal sinus (SSS) in animal models of migraines [31]. Furthermore, AMI profoundly blocked $Na_v1.8$ currents in concentration-, use- and state-dependent manners in acute isolated TG neurons (unpublished data). In the present study, the effects of AMI on the biophysical properties of $Na_v1.9$ currents in acute isolated TG neurons were examined using whole-cell patch clamp recordings, which may provide a new molecular basis for the analgesic action of AMI.

Results

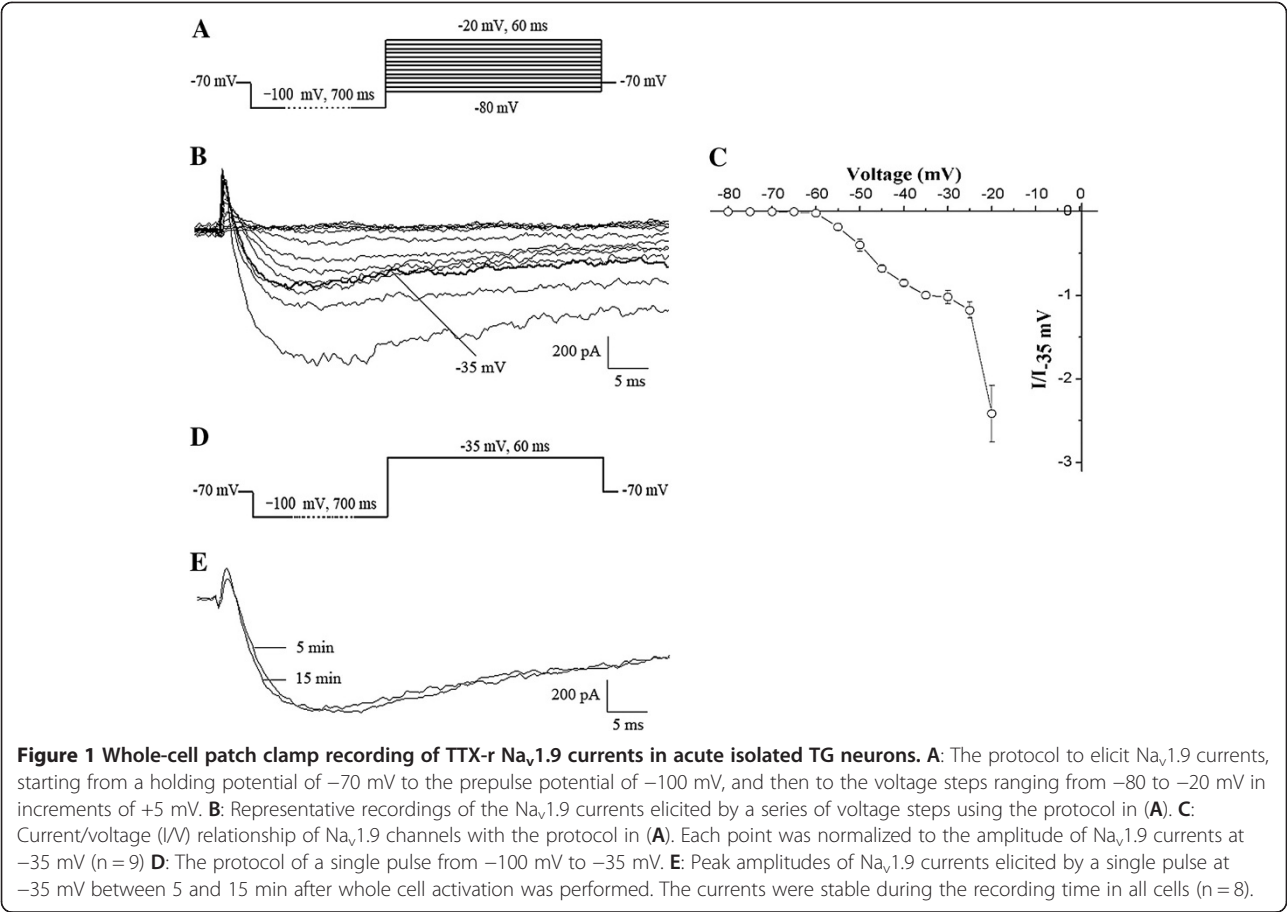### Recording of $Na_v1.9$ currents in acute isolated TG neurons

In the present study, whole-cell voltage recordings were only performed on small-sized TG neurons (15–23 μm), which served as nociceptors [32]. Of 209 total neurons, 125 that showed stable recording conditions before and after compound application and washout were included for further study. According to a previous report [19,23], a voltage-clamp protocol in which neurons hyperpolarized over the course of 700 ms in response to the application of −100 mV before voltage steps applied (see protocol in Figure 1A) was used to elicit TTX-r $Na_v1.9$ currents in the presence of 500 nM TTX. This step-wise protocol activated $Na_v1.9$ currents first at approximately −60 mV, followed by $Na_v1.8$ currents from −30 to −20 mV. Although $Na_v1.8$ currents were greatest, the presence of $Na_v1.9$ produced a prominent shoulder (around −35 mV) on the current/voltage (I/V) curve (Figure 1C), which before performing further experiment was examined in every TG neuron to exclude cells that do not express $Na_v1.9$. Therefore, TTX-r Na^+ currents at voltages ranging from −60 to −35 mV were mainly mediated by $Na_v1.9$ channels, and the single voltage step at −35 mV was chosen to elicit the peak amplitude of $Na_v1.9$ currents. The above properties are in agreement with $Na_v1.9$ currents that were previously characterized in rat DRG neurons [19,23]. To observe the stabilization of its peak amplitude, $Na_v1.9$ currents elicited by −35 mV were measured after whole-cell stimulation was performed. As shown in Figure 1E, the peak amplitude of $Na_v1.9$ currents was relatively stable from 5 to 15 min (n = 8). All of our subsequent experiments were recorded during this time.

Effect of different concentrations of AMI on $Na_v1.9$ currents

A single voltage step protocol was used to evaluate the effect of AMI on $Na_v1.9$ currents in rat TG neurons (Figure 2A). AMI caused concentration-dependent decreases in peak amplitudes of $Na_v1.9$ currents, and these effects were partially reversed when AMI was washed away (Figure 2B). AMI inhibition was significant at all the following concentrations except 0.1 μM: 0.1 μM ($1.01 \pm 2.98\%$; n = 9, $P > 0.05$), 1 μM ($15.84 \pm 2.42\%$; n = 7, $P < 0.05$), 5 μM ($37.11 \pm 3.51\%$; n = 9, $P < 0.05$), 10 μM ($42.19 \pm 3.28\%$; n = 8, $P < 0.05$), 50 μM ($65.28 \pm 7.41\%$; n = 9, $P < 0.05$) and 100 μM ($81.00 \pm 5.20\%$; n = 6, $P < 0.05$) (Figure 2C). Fitting to the Hill equation revealed a half-blockade (IC_{50}) at 15.16 μM with an apparent Hill coefficient of 0.64.
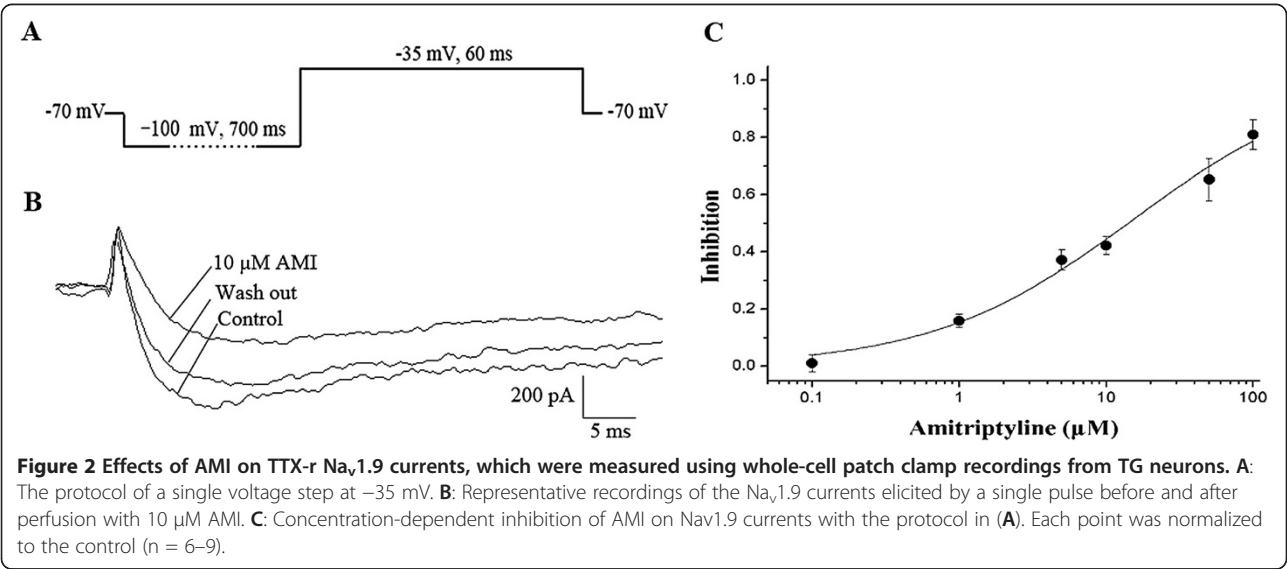
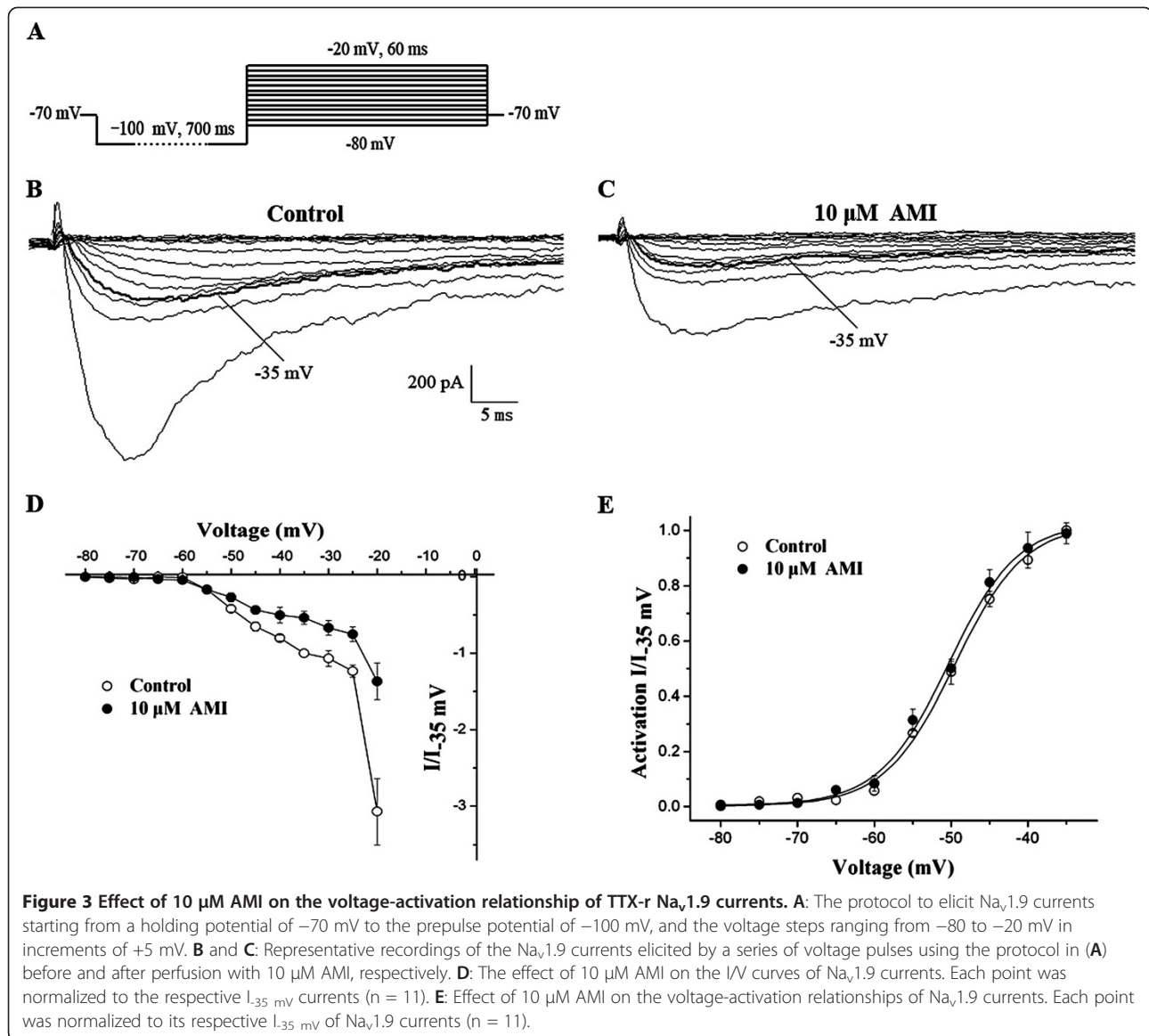### Effect of AMI on $Na_v1.9$ channel activation

To examine the effects of AMI on channel activation kinetics, $Na_v1.9$ currents were evoked by hyperpolarizing

Figure 1 Whole-cell patch clamp recording of TTX-r Na$_v$1.9 currents in acute isolated TG neurons. A: The protocol to elicit Na$_v$1.9 currents, starting from a holding potential of −70 mV to the prepulse potential of −100 mV, and then to the voltage steps ranging from −80 to −20 mV in increments of +5 mV. **B**: Representative recordings of the Na$_v$1.9 currents elicited by a series of voltage steps using the protocol in (**A**). **C**: Current/voltage (I/V) relationship of Na$_v$1.9 channels with the protocol in (**A**). Each point was normalized to the amplitude of Na$_v$1.9 currents at −35 mV (n = 9) **D**: The protocol of a single pulse from −100 mV to −35 mV. **E**: Peak amplitudes of Na$_v$1.9 currents elicited by a single pulse at −35 mV between 5 and 15 min after whole cell activation was performed. The currents were stable during the recording time in all cells (n = 8).

cells to −100 mV over the course of 700 ms, followed by the application of voltage steps ranging from −80 to −20 mV in increments of +5 mV (Figure 3A). Figures 3B and 3C show typical I/V relationships before and after perfusion with 10 μM AMI, respectively. The I/V curve

was shifted upward after exposure to 10 μM AMI (Figure 3D). However, the voltage-activation curve that was fitted to the Boltzman equation only exhibited a slightly hyperpolarization after perfusion with 10 μM AMI (Figure 3E). The voltage generating half-maximal

Figure 2 Effects of AMI on TTX-r Na$_v$1.9 currents, which were measured using whole-cell patch clamp recordings from TG neurons. A: The protocol of a single voltage step at −35 mV. **B**: Representative recordings of the Na$_v$1.9 currents elicited by a single pulse before and after perfusion with 10 μM AMI. **C**: Concentration-dependent inhibition of AMI on Nav1.9 currents with the protocol in (**A**). Each point was normalized to the control (n = 6–9).

Figure 3 Effect of 10 μM AMI on the voltage-activation relationship of TTX-r Na$_v$1.9 currents. A: The protocol to elicit Na$_v$1.9 currents starting from a holding potential of −70 mV to the prepulse potential of −100 mV, and the voltage steps ranging from −80 to −20 mV in increments of +5 mV. **B** and **C**: Representative recordings of the Na$_v$1.9 currents elicited by a series of voltage pulses using the protocol in (**A**) before and after perfusion with 10 μM AMI, respectively. **D**: The effect of 10 μM AMI on the I/V curves of Na$_v$1.9 currents. Each point was normalized to the respective I$_{-35\ mV}$ currents (n = 11). **E**: Effect of 10 μM AMI on the voltage-activation relationships of Na$_v$1.9 currents. Each point was normalized to its respective I$_{-35\ mV}$ of Na$_v$1.9 currents (n = 11).

current (V$_{0.5act}$) was −49.58 ± 0.49 mV before and −50.36 ± 0.53 mV after perfusion with 10 μM AMI (n = 11, $P > 0.05$), and the slop factor k did not change significantly (4.55 ± 0.43 before to 4.51 ± 0.47 after perfusion with 10 μM AMI, $P > 0.05$).

Effect of AMI on Na$_v$1.9 channel inactivation

To measure the steady-state inactivation of Na$_v$1.9 channels, double-pulse protocols starting from a holding potential of −70 mV were used. Conditioning pulses from −110 mV to −35 mV were performed over 1 s to ensure that Na$_v$1.9 channels were entirely inactivated (Figure 4A). Figures 4B and C show the recorded channel responses to test pulses (the voltage step at −35 mV for 200 ms) before and after exposure to 10 μM AMI, respectively. The steady-state inactivation, fit to the Boltzmann equation

exhibited a significant hyperpolarization (Figure 4D). Half-maximal steady-state inactivation (V$_{0.5inact}$) was −54.50 ± 0.77 mV before and −64.17 ± 1.09 mV after perfusion with 10 μM AMI (n = 11, $P < 0.05$), and there was no statistical change in the slop factor k (8.47 ± 0.56 before to 8.86 ± 0.92 after perfusion with 10 μM AMI, $P > 0.05$).

Effect of AMI on use-dependent blockade of Na$_v$1.9 channels

To study whether its channels could be blocked by AMI in use-dependent manner, Na$_v$1.9 channels were activated at 1 Hz by 60 test pulses at −35 mV from a hyperpolarized potential of −100 mV (Figure 5A). Treatment with 10 μM AMI significantly reduced the peak amplitude of Na$_v$1.9 currents compared to those in the absence of AMI (Figure 5B); however, AMI had little
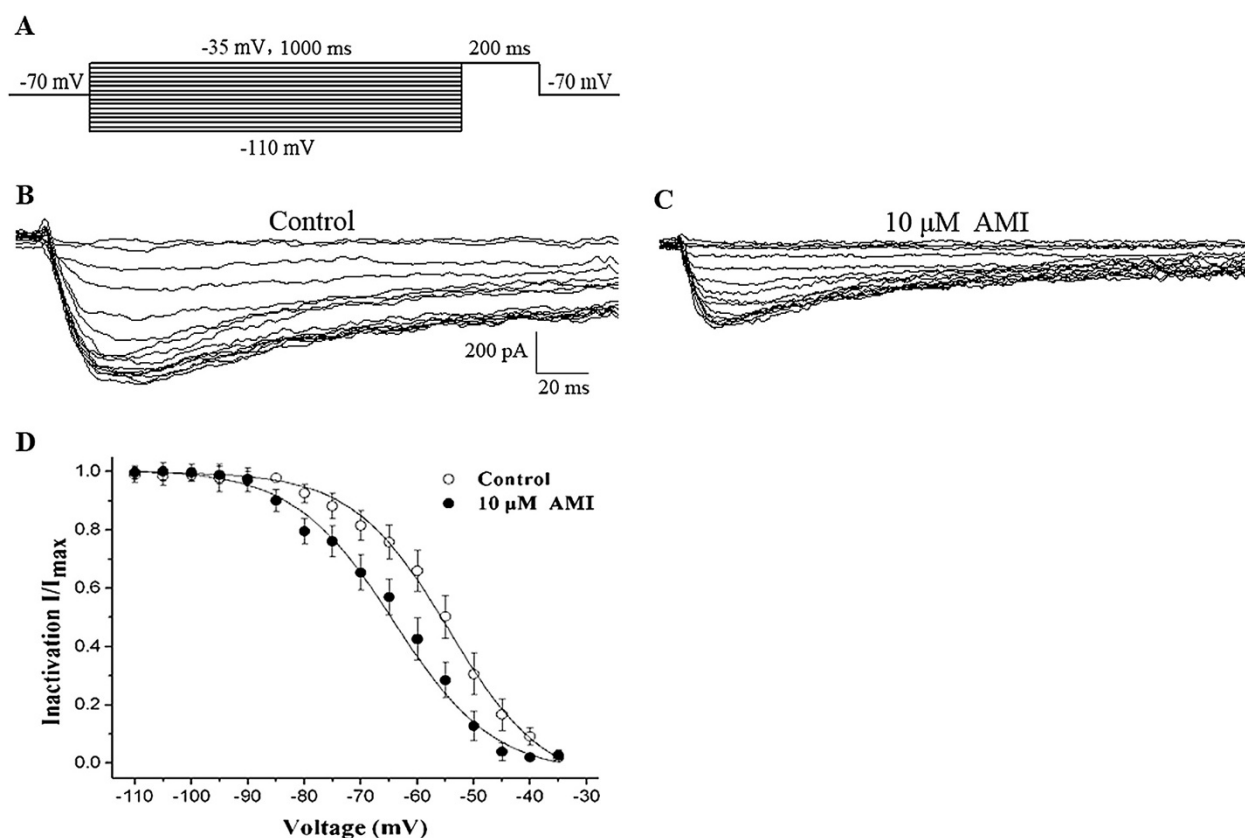
Figure 4 Effect of 10 μM AMI on the steady-state inactivation relationship of TTX-r Na$_v$1.9 currents. A: The protocol to elicit steady-state inactivation of Na$_v$1.9 currents starting from a holding potential of −70 mV, applying conditioning pulses ranging from −110 to −35 mV in increments of +5 mV, and applying a test pulse at −35 mV. **B** and **C**: Representative recordings of the Na$_v$1.9 currents elicited by a series of test pulses using the protocol in (**A**) before and after exposure to 10 μM AMI, respectively. **D**: The effect of 10 μM AMI on the steady-state inactivation relationship of Na$_v$1.9 currents. Each point was normalized to its respective maximal Na$_v$1.9 currents (n = 11).

effect on the use-dependence of Na$_v$1.9 channels (Figure 5C). The amplitude of the 60th Na$_v$1.9 current only slightly decreased to $94.29 \pm 2.50\%$ of the first current during the 10 μM AMI perfusion, and no difference was observed when compared to control currents ($97.13 \pm 2.26\%$, n = 9, $P > 0.05$; Figure 5E). To rule out the influence of the concentration on use-dependent blockade, 50 μM AMI was used in a subsequent test. Similar to the 10 μM experiments, 50 μM AMI had little effect on the use-dependence of Na$_v$1.9 channels ($93.65 \pm 1.43\%$ of the first one, n = 9; Figures 5D and 5E). These results indicated that AMI did not significantly contribute to the use-dependent blockade of Na$_v$1.9 currents when stimulated by 60 pulses at 1 Hz.

Discussion

Although AMI has been widely reported to block some subtypes of VGSCs, including Na$_v$1.5, Na$_v$1.7 and Na$_v$1.8 [11,16], to our knowledge, this is the first report that

studies the effects of AMI on TTX-r Na$_v$1.9 channels in TG neurons.

The present results showed that AMI efficiently inhibited Na$_v$1.9 channels in rat TG neurons in a concentration-dependent manner and had an IC$_{50}$ of 15.16 μM, consistent with previous findings that AMI blocked TTX-r Na$^+$ currents in rat TG neurons (IC$_{50}$ of AMI was 15.8 μM) [17]. In patients with depression or neuropathic pain who receive daily doses of 10 to 300 mg AMI, plasma steady-state concentrations range from 0.36 to 0.90 μM [33]. The concentrations of AMI used in this study are higher than the clinically relevant plasma concentrations. However, even at clinically relevant concentrations between 0.1 and 1 μM, the peak Na$^+$ currents were still decreased by approximately 1–15%. However, the brain and plasma concentration ratios of AMI observed in chronically treated rats were found to be more than 20:1, which was similar to levels reported in humans [34,35]. In this case, the IC$_{50}$ value for Na$_v$1.9 channels would be similar to the concentration of AMI found in the brain: it is thus possible that Na$_v$1.9 channels

Figure 5 Effect of 10 and 50 μM AMI on the use-dependent relationship of TTX-r Na$_v$1.9 currents. A: The protocol of a single voltage step at −35 mV. **B**, **C** and **D**: Representative recordings of the Na$_v$1.9 currents elicited by 60 pulses at 1 Hz before and after perfusion with 10 and 50 μM AMI, respectively. **E**: The effect of 10 and 50 μM AMI on the use-dependent relationship of Na$_v$1.9 currents. Each point was normalized to the respective first Na$_v$1.9 current (n = 9). **F**: The current at the 60th pulse normalized to the current of the first pulse, was not significantly decreased after perfusion with 10 or 50 μM AMI compared to that of the controls (n = 9, P > 0.05).

are effectively inhibited in TG neurons. Unlike drugs that block both TTX-s and TTX-r Na$^+$ channels in rat DRG neurons by modulating Na$^+$ channel activation and inactivation kinetics [15], AMI produced only a prominent hyperpolarizing shift in the steady-state inactivation curves of Na$_v$1.9 channels and had no significant effects on the channel activation kinetics in rat TG neurons, indicating that the binding of AMI to Na$_v$1.9 channels was state-dependent. This phenomenon was similar to previous reports on the inhibition of TTX-r Na$^+$ channels in rat TG neurons [17]. The discrepancy in these findings may be due to differences in tissue sources and the experimental protocols.

Previous studies have shown that the blockade of TTX-s and TTX-r Na$^+$ channels and Na$_v$1.8 channels by local anesthetics and AMI is highly use-dependent [16,36,37]. However, there was no use-dependent blockade in the presence of 10 or 50 μM AMI at 1 Hz stimulation in this study. This use-dependent blockade would

result from the binding of an antagonist ligand to inactivated channels that are more prevalent during repetitive stimulation and from the dissociation of the antagonist from the inactivated states with a time constant slower than the frequency of the pulses, which means that use-dependent blockade arises from the slow recovery of antagonist-bound channels due to an interaction between antagonist and inactivated states [16,37]. According to this hypothesis, the dissociation time constant of AMI from inactivated Na$_v$1.9 channels might be faster than the frequency of the pulses (1 Hz) used in this study. Clearly, only one frequency was tested in this experiment; higher frequencies, such as 5, 10 or 20 Hz, were not investigated due to limitations in the protocol, in which the spent time of a single voltage step was approximately 900 ms (Figure 5A). These inconsistent findings might also be explained by the presence of the different binding sites. For example, local anesthetics and AMI are known to block Na$_v$1.8 channels in a use-

dependent manner by binding to the same binding site, which are located within the ion-conducting pore [8,38,39]. Selective $Na_v1.8$ channel blockers A-803467 and A-887826 do not cause use-dependent blockage and were instead thought to recognize a binding site that is distinct from the binding sites for use-dependent blockers [40]. It was recently proposed that $Na_v1.9$ currents exhibit ultraslow activation and inactivation kinetics, which is likely the product of a substantially different amino acid sequence, especially in the voltage-sensing regions, compared to other Na^+ channel subtypes [22,41]. Therefore, further studies on the dissociation time constant of AMI from the inactivated states of $Na_v1.9$ channels will help address this issue.

In addition to having the effect on $Na_v1.9$ currents in the present study, AMI was also reported to inhibit $Na_v1.8$ channels heterologously expressed in ND7/23 cells in concentration- and use-dependent manners, and to change activation and inactivation kinetics of $Na_v1.8$ channels [16]. Similar results were also obtained from our study on modulation of $Na_v1.8$ channels by AMI in TG neurons (unpublished data). $Na_v1.8$ and $Na_v1.9$ channels may be individually expressed or co-expressed in the small diameter TG neurons, so the potential contamination with $Na_v1.8$ current and possible impact on AMI behavior may be included in the present study, although $Na_v1.8$ and $Na_v1.9$ currents can be distinguished by the experimental protocols [19,23] and the I/V curve which was examined in every TG neuron to validate presence of $Na_v1.9$. This study showed that AMI had no effects on the activation kinetics and had no use-dependent blockade of $Na_v1.9$. However, it is well documented that AMI significantly changed the activation kinetics and caused use-dependent blockade of $Na_v1.8$ [16]. These results suggested that even if it had, it would only a little the potential contamination with $Na_v1.8$ current and a little impact on AMI behavior in the present study.

Persistent subthreshold Na^+ currents, carried primarily by $Na_v1.9$ channels that are expressed exclusively in small nociceptive TG and DRG neurons [27-30], are known to lessen spike threshold and eventually facilitate maintained spiking [23,42]. The loss of $Na_v1.9$-mediated Na^+ currents was associated with the inability of neurons to generate a large variety of electrophysiological behaviors, including subthreshold regenerative depolarization, active hyperpolarizing responses, oscillatory bursting discharges, plateau potentials and bistable membranes [43]. In $Na_v1.9$ knock-out mice, there is a loss of persistent currents and blunted or missing pain behaviors induced by complete Freund adjuvant (CFA), carrageenan, formalin, and prostaglandin E2 (PGE2) [44] or in response to inflammatory mediators, such as bradykinin, serotonin, interleukin-1beta, and P2X3 and

P2Y receptor agonists [45]. Consistently, antisense-based $Na_v1.9$ gene silencing in rats attenuated carrageenan-induced heat and mechanical pain allodynia [46]. Response to pain is relevant to the persistent currents, as demonstrated by electrophysiological studies in isolated primary sensory neurons, where inflammatory mediators such as PGE2 and serotonin [44,47], as well as some secreted proteins (e.g., glial-derived neurotrophic factor (GDNF) [48]), or activators of G protein pathways [26], have been reported to increase $Na_v1.9$ currents.

Migraines are the most common headache disorder and affect more than 10% of the general population [49,50]. Migraines are thought to arise from the activation and sensitization of the trigeminovascular system, followed by the release of inflammatory mediators from the trigeminal system, with a consequent vasodilation of innervate intracranial blood vessels and generation of neurogenic inflammation [51]. Such inflammation causes hyperexcitability of TG neurons (peripheral sensitization) and the second-order sensory neurons (central sensitization) [52,53]. The above-mentioned PGE2, interleukin-1 beta, and G protein-coupled P2X3 and P2Y receptors, which are known to functionally regulate $Na_v1.9$ channels during inflammation, have also been closely linked to the pathophysiology of migraines in a variety of experimental and clinical studies [54-57]. In addition, immunohistochemical experiments had shown that P2X3, bradykinin B2, and transient receptor potential vanilloid 1 (TRPV1) receptors are highly co-localized with $Na_v1.9$ channels in nociceptor sensory neurons [45]. TRPV1 receptors have been implicated as new therapeutic targets for the treatment of migraines [58]. Although there is not a direct link between migraines and $Na_v1.9$ channels, AMI has been widely used for the prophylactic treatment of migraines and has demonstrated clear success in clinical practice. These results were supported by our findings that AMI efficiently blocked $Na_v1.9$ currents, which might help, at least in part, understand the mechanism underlying AMI efficacy in migraine pain.

Conclusion
In summary, the present results demonstrate that AMI is a state-selective blocker of $Na_v1.9$ channels in nociceptive trigeminal neurons, which likely contributes to the analgesic action of AMI in various pains including migraines.

Methods
Preparation of TG neurons
All experimental procedures were approved by the Committee of Animal Use for Research and Education of the Laboratory Animals Center of the Chinese PLA

General Hospital (Beijing, PR China) and were consistent with the ethical guidelines recommended by the International Association for the Study of Pain in conscious animals [59]. Efforts were made to minimize the animals' suffering. TG neurons from 7-day-old neonatal Sprague–Dawley rats (The Academy of Military Medical Sciences, Beijing, PR China) were prepared using a modified version of a previously described method [60]. Briefly, rats were deeply anesthetized by intraperitoneal injection of euthasol (0.1 mg/kg) and decapitated. A pair of the TGs were rapidly dissected from each animal, washed several times in ice-cold Hank's Balanced Salt Solution (HBSS; Life Technology, MD), and then dissociated by mechanical disruption and incubated in 2 mL HBSS containing 0.25% trypsin at 37℃ for 25 min. The tissues were washed twice in DMEM (high glucose) (Hyclone, Logan, UT) and resuspended in DMEM with 10% fetal bovine serum, 10% heat-inactivated horse serum and 1% L-glutamine, and triturated with a flame-polished Pasteur pipette to dissociate individual cells. Subsequently, cells were plated onto poly-L-lysine-coated glass coverslips (12 mm diameter) placed in 24-well plates, and then maintained in a humidified atmosphere of 95% air and 5% CO_2 at 37℃. The cells were used for recordings between 2 and 10 h after plating.

Patch clamp recordings

The whole-cell patch clamp recordings were performed at room temperature; currents were measured with an Axopatch-200B (Axon Instruments, Inc., Foster City, CA, USA) and recorded with pClamp 8.2 software (Axon Instruments, Inc., Foster City, CA, USA). The output was digitized with a Digidata 1322A converter (Axon Instruments, Inc., Foster City, CA, USA). Patch pipettes were made by a two-step vertical puller (Narishige Scientific Instrument Laboratory, Tokyo, Japan; model PP-83) from borosilicate glass and had resistances between 2 to 3 MΩ after perfusion of internal solution through the pipette. Cells in the glass coverslip dishes were placed in a recording chamber and visualized with the phase contrast microscopy on an inverted microscope (Nikon, Tokyo, Japan). Currents were recorded from small TG neurons (15–23 μm diameter). Experiments were performed at a holding potential of –70 mV for $Na_v1.9$ currents. After gigaohm seal formation and membrane disruption, the whole cell capacitance was cancelled and series resistance was compensated for (> 80%). Data were low-pass-filtered at 2 kHz, sampled at 10 kHz, and acquired with the pulse protocol. The liquid junction potential between internal and external solutions was –5 mV on average and was used to correct for the recorded membrane potential. The pipette solution was composed of the following (in mM): 140 CsCl, 10 NaCl, 1 MgCl•$6H_2O$, 0.5 $CaCl_2$, 5 EGTA, 10 HEPES and 2 Na_2-ATP, and adjusted to

pH 7.4 with CsOH (320 mosm). Extracellular solution contained the following (in mM): 120 NaCl, 5 KCl, 30 TEA-Cl, 10 Glucose, 10 HEPES, 10 4-AP, 2 $CaCl_2$, 0.1 $CdCl_2$, 2 MgCl•$6H_2O$ and 0.0005 TTX, and adjusted to pH 7.4 with NaOH (310 mosm). The TEA-Cl, $CdCl_2$ and TTX were used to inhibit endogenous K^+, Ca^{2+} and TTX-s sodium currents, respectively.

Drugs and chemicals used

AMI, TTX, trypsin, L-glutamine, poly-L-lysine, HEPES, EGTA, TEA-Cl, Na_2-ATP, $CdCl_2$, CsOH and CsCl were purchased from Sigma. Other chemical reagents used were of analytic grade. AMI was prepared as a 100 mM stock solution in distilled water and further dilutions were made fresh in extracellular solution on the day of each experiment. AMI was continuously administered (approximately 1 mL/min) to the cells via superfusion polyethylene tubes during the recording procedure.

Data analysis

Data were analyzed using pCLAMP 10.0 (Axon instruments, USA) and Origin 7.5 (Microcal Software, Northampton, MA, USA) software. Concentration-response curves were fit to the Hill function: $I_{drug}/I_{control} = 1/[1 + (C/IC_{50})^H]$, where $I_{drug}/I_{control}$ is fractional blockade, C is the drug concentration, IC_{50} is the drug concentration that causes 50% blockade, and H is the Hill coefficient. The voltage-activation curves and the steady-state inactivation curves were fit with the Boltzmann function: $I/I_{max} = 1 – 1/(1 + \exp[(V_m – V_{0.5\ act})/k)]$ and $I/I_{max} = 1/(1 + \exp[(V_m – V_{0.5\ inact})/k)]$, respectively, where Imax is maximal current, V_m is the prepulse voltage, $V_{0.5}$ is the voltage generating half maximal current, and k is the slope factor of the curves. All data are presented as the mean ± SEM. Statistical significance was assessed using SPSS 13.0 (SPSS Inc, Chicago, IL). Student's t-test analysis was used to assess differences between means from two groups. One-way ANOVA of variance followed by Dunnett post-testing was performed to assess differences than two more groups. A P value < 0.05 was considered to be significant.

Authors' contributions

JYL and XYL performed the patch clamp recordings in TG neurons. JQZ was partially involved in experimental design and guiding. SYY is the corresponding author. All authors read and approved the final manuscript.

Author details

[1]Department of Neurology, Chinese PLA General Hospital, Beijing 100853, PR China. [2]Department of Biochemical Pharmacology, Beijing Institute of Pharmacology and Toxicology, Beijing 100850, PR China.

References

1. Wong MC, Chung JW, Wong TK: **Effects of treatments for symptoms of painful diabetic neuropathy: systematic review.** *BMJ* 2007, **335**:87.
2. Smitherman TA, Walters AB, Maizels M, Penzien DB: **The use of antidepressants for headache prophylaxis.** *CNS Neurosci Ther* 2011, **17**:462–469.
3. Coluzzi F, Mattia C: **Mechanism-based treatment in chronic neuropathic pain: the role of antidepressants.** *Curr Pharm Des* 2005, **11**:2945–2960.
4. Onghena P, Van Houdenhove B: **Antidepressant-induced analgesia in chronic non-malignant pain: a meta-analysis of 39 placebo-controlled studies.** *Pain* 1992, **49**:205–219.
5. Mao QX, Yang TD: **Amitriptyline upregulates EAAT1 and EAAT2 in neuropathic pain rats.** *Brain Res Bull* 2010, **81**:424–427.
6. Dick IE, Brochu RM, Purohit Y, Kaczorowski GJ, Martin WJ, Priest BT: **Sodium channel blockade may contribute to the analgesic efficacy of antidepressants.** *J Pain* 2007, **8**:315–324.
7. Gerner P, Srinivasa V, Zizza AM, Zhuang ZY, Luo S, Zurakowski D, Eappen S, Wang G: **Doxepin by topical application and intrathecal route in rats.** *Anesth Analg* 2006, **102**:283–287.
8. Brau ME, Dreimann M, Olschewski A, Vogel W, Hempelmann G: **Effect of drugs used for neuropathic pain management on tetrodotoxin-resistant Na(+) currents in rat sensory neurons.** *Anesthesiology* 2001, **94**:137–144.
9. Sudoh Y, Cahoon EE, Gerner P, Wang GK: **Tricyclic antidepressants as long-acting local anesthetics.** *Pain* 2003, **103**:49–55.
10. Catterall WA, Goldin AL, Waxman SG: **International Union of Pharmacology. XLVII. Nomenclature and structure-function relationships of voltage-gated sodium channels.** *Pharmacol Rev* 2005, **57**:397–409.
11. Thorstrand C, Bergstrom J, Castenfors J: **Cardiac effects of amitriptyline in rats.** *Scand J Clin Lab Invest* 1976, **36**:7–15.
12. Ishii Y, Sumi T: **Amitriptyline inhibits striatal efflux of neurotransmitters via blockade of voltage-dependent Na + channels.** *Eur J Pharmacol* 1992, **221**:377–380.
13. Pancrazio JJ, Kamatchi GL, Roscoe AK, Lynch C 3rd: **Inhibition of neuronal Na + channels by antidepressant drugs.** *J Pharmacol Exp Ther* 1998, **284**:208–214.
14. Yan L, Wang Q, Fu Q, Ye Q, Xiao H, Wan Q: **Amitriptyline inhibits currents and decreases the mRNA expression of voltage-gated sodium channels in cultured rat cortical neurons.** *Brain Res* 2010, **1336**:1–9.
15. Song JH, Ham SS, Shin YK, Lee CS: **Amitriptyline modulation of Na(+) channels in rat dorsal root ganglion neurons.** *Eur J Pharmacol* 2000, **401**:297–305.
16. Leffler A, Reiprich A, Mohapatra DP, Nau C: **Use-dependent block by lidocaine but not amitriptyline is more pronounced in tetrodotoxin (TTX)-Resistant Nav1.8 than in TTX-sensitive Na + channels.** *J Pharmacol Exp Ther* 2007, **320**:354–364.
17. Hur YK, Choi IS, Cho JH, Park EJ, Choi JK, Choi BJ, Jang IS: **Effects of carbamazepine and amitriptyline on tetrodotoxinresistant Na + channels in immature rat trigeminal ganglion neurons.** *Arch Pharm Res* 2008, **31**:178–182.
18. Akopian AN, Sivilotti L, Wood JN: **A tetrodotoxin-resistant voltage-gated sodium channel expressed by sensory neurons.** *Nature* 1996, **379**:257–262.
19. Ebersberger A, Natura G, Eitner A, Halbhuber KJ, Rost R, Schaible HG: **Effects of prostaglandin D2 on tetrodotoxin-resistant Na + currents in DRG neurons of adult rat.** *Pain* 2011, **152**:1114–1126.
20. Roy ML, Narahashi T: **Differential properties of tetrodotoxin-sensitive and tetrodotoxin-resistant sodium channels in rat dorsal root ganglion neurons.** *J Neurosci* 1992, **12**:2104–2111.
21. Dib-Hajj S, Black JA, Cummins TR, Waxman SG: **NaN/Nav1.9: a sodium channel with unique properties.** *Trends Neurosci* 2002, **25**:253–259.
22. Cummins TR, Dib-Hajj SD, Black JA, Akopian AN, Wood JN, Waxman SG: **A novel persistent tetrodotoxin-resistant sodium current in SNS-null and wild-type small primary sensory neurons.** *J Neurosci* 1999, **19**:RC43.
23. Coste B, Osorio N, Padilla F, Crest M, Delmas P: **Gating and modulation of presumptive NaV1.9 channels in enteric and spinal sensory neurons.** *Mol Cell Neurosci* 2004, **26**:123–134.
24. Renganathan M, Cummins TR, Waxman SG: **Contribution of Na(v)1.8 sodium channels to action potential electrogenesis in DRG neurons.** *J Neurophysiol* 2001, **86**:629–640.
25. Rush AM, Cummins TR, Waxman SG: **Multiple sodium channels and their roles in electrogenesis within dorsal root ganglion neurons.** *J Physiol* 2007, **579**:1–14.
26. Ostman JA, Nassar MA, Wood JN, Baker MD: **GTP up-regulated persistent Na + current and enhanced nociceptor excitability require NaV1.9.** *J Physiol* 2008, **586**:1077–1087.
27. Amaya F, Decosterd I, Samad TA, Plumpton C, Tate S, Mannion RJ, Costigan M, Woolf CJ: **Diversity of expression of the sensory neuron-specific TTX-resistant voltage-gated sodium ion channels SNS and SNS2.** *Mol Cell Neurosci* 2000, **15**:331–342.
28. Eriksson J, Jablonski A, Persson AK, Hao JX, Kouya PF, Wiesenfeld-Hallin Z, Xu XJ, Fried K: **Behavioral changes and trigeminal ganglion sodium channel regulation in an orofacial neuropathic pain model.** *Pain* 2005, **119**:82–94.
29. Djouhri L, Fang X, Okuse K, Wood JN, Berry CM, Lawson SN: **The TTX-resistant sodium channel Nav1.8 (SNS/PN3): expression and correlation with membrane properties in rat nociceptive primary afferent neurons.** *J Physiol* 2003, **550**:739–752.
30. Fang X, Djouhri L, McMullan S, Berry C, Waxman SG, Okuse K, Lawson SN: **Intense isolectin-B4 binding in rat dorsal root ganglion neurons distinguishes C-fiber nociceptors with broad action potentials and high Nav1.9 expression.** *J Neurosci* 2006, **26**:7281–7292.
31. Liang J, Yu S, Dong Z, Wang X, Liu R, Chen X, Li Z: **The effects of OB-induced depression on nociceptive behaviors induced by electrical stimulation of the dura mater surrounding the superior sagittal sinus.** *Brain Res* 2011, **1424**:9–19.
32. Fang Z, Park CK, Li HY, Kim HY, Park SH, Jung SJ, Kim JS, Monteil A, Oh SB, Miller RJ: **Molecular basis of Ca(v)2.3 calcium channels in rat nociceptive neurons.** *J Biol Chem* 2007, **282**:4757–4764.
33. Wang GK, Russell C, Wang SY: **State-dependent block of voltage-gated Na + channels by amitriptyline via the local anesthetic receptor and its implication for neuropathic pain.** *Pain* 2004, **110**:166–174.
34. Glotzbach RK, Preskorn SH: **Brain concentrations of tricyclic antidepressants: single-dose kinetics and relationship to plasma concentrations in chronically dosed rats.** *Psychopharmacology (Berl)* 1982, **78**:25–27.
35. Karson CN, Newton JE, Livingston R, Jolly JB, Cooper TB, Sprigg J, Komoroski RA: **Human brain fluoxetine concentrations.** *J Neuropsychiatry Clin Neurosci* 1993, **5**:322–329.
36. John VH, Main MJ, Powell AJ, Gladwell ZM, Hick C, Sidhu HS, Clare JJ, Tate S, Trezise DJ: **Heterologous expression and functional analysis of rat Nav1.8 (SNS) voltage-gated sodium channels in the dorsal root ganglion neuroblastoma cell line ND7–23.** *Neuropharmacology* 2004, **46**:425–438.
37. Ong BH, Tomaselli GF, Balser JR: **A structural rearrangement in the sodium channel pore linked to slow inactivation and use dependence.** *J Gen Physiol* 2000, **116**:653–662.
38. Barber MJ, Starmer CF, Grant AO: **Blockade of cardiac sodium channels by amitriptyline and diphenylhydantoin. Evidence for two use-dependent binding sites.** *Circ Res* 1991, **69**:677–696.
39. Nau C, Wang GK: **Interactions of local anesthetics with voltage-gated Na + channels.** *J Membr Biol* 2004, **201**:1–8.
40. Zhang XF, Shieh CC, Chapman ML, Matulenko MA, Hakeem AH, Atkinson RN, Kort ME, Marron BE, Joshi S, Honore P, *et al*: **A-887826 is a structurally novel, potent and voltage-dependent Na(v)1.8 sodium channel blocker that attenuates neuropathic tactile allodynia in rats.** *Neuropharmacology* 2010, **59**:201–207.
41. Gilchrist J, Bosmans F: **Animal toxins can alter the function of Nav1.8 and Nav1.9.** *Toxins (Basel)* 2012, **4**:620–632.
42. Crill WE: **Persistent sodium current in mammalian central neurons.** *Annu Rev Physiol* 1996, **58**:349–362.

43. Maingret F, Coste B, Padilla F, Clerc N, Crest M, Korogod SM, Delmas P: Inflammatory mediators increase Nav1.9 current and excitability in nociceptors through a coincident detection mechanism. *J Gen Physiol* 2008, **131**:211–225.

44. Priest BT, Murphy BA, Lindia JA, Diaz C, Abbadie C, Ritter AM, Liberator P, Iyer LM, Kash SF, Kohler MG, *et al*: Contribution of the tetrodotoxin-resistant voltage-gated sodium channel NaV1.9 to sensory transmission and nociceptive behavior. *Proc Natl Acad Sci USA* 2005, **102**:9382–9387.

45. Amaya F, Wang H, Costigan M, Allchorne AJ, Hatcher JP, Egerton J, Stean T, Morisset V, Grose D, Gunthorpe MJ, *et al*: The voltage-gated sodium channel Na(v)1.9 is an effector of peripheral inflammatory pain hypersensitivity. *J Neurosci* 2006, **26**:12852–12860.

46. Lolignier S, Amsalem M, Maingret F, Padilla F, Gabriac M, Chapuy E, Eschalier A, Delmas P, Busserolles J: Nav1.9 channel contributes to mechanical and heat pain hypersensitivity induced by subacute and chronic inflammation. *PLoS One* 2011, **6**:e23083.

47. Rush AM, Waxman SG: PGE2 increases the tetrodotoxin-resistant Nav1.9 sodium current in mouse DRG neurons via G-proteins. *Brain Res* 2004, **1023**:264–271.

48. Cummins TR, Black JA, Dib-Hajj SD, Waxman SG: Glial-derived neurotrophic factor upregulates expression of functional SNS and NaN sodium channels and their currents in axotomized dorsal root ganglion neurons. *J Neurosci* 2000, **20**:8754–8761.

49. Andlin-Sobocki P, Jonsson B, Wittchen HU, Olesen J: Cost of disorders of the brain in Europe. *Eur J Neurol* 2005, **12**(Suppl 1):1–27.

50. Yu S, Liu R, Zhao G, Yang X, Qiao X, Feng J, Fang Y, Cao X, He M, Steiner T: The prevalence and burden of primary headaches in China: a population-based door-to-door survey. *Headache* 2012, **52**:582–591.

51. Pietrobon D: Migraine: new molecular mechanisms. *Neuroscientist* 2005, **11**:373–386.

52. Burstein R: Deconstructing migraine headache into peripheral and central sensitization. *Pain* 2001, **89**:107–110.

53. Wu W, Ye Q, Wang W, Yan L, Wang Q, Xiao H, Wan Q: Amitriptyline modulates calcium currents and intracellular calcium concentration in mouse trigeminal ganglion neurons. *Neurosci Lett* 2012, **506**:307–311.

54. Antonova M, Wienecke T, Olesen J, Ashina M: Prostaglandin E(2) induces immediate migraine-like attack in migraine patients without aura. *Cephalalgia* 2012, **32**:822–833.

55. Neeb L, Hellen P, Boehnke C, Hoffmann J, Schuh-Hofer S, Dirnagl U, Reuter U: IL-1beta stimulates COX-2 dependent PGE(2) synthesis and CGRP release in rat trigeminal ganglia cells. *PLoS One* 2011, **6**:e17360.

56. Giniatullin R, Nistri A, Fabbretti E: Molecular mechanisms of sensitization of pain-transducing P2X3 receptors by the migraine mediators CGRP and NGF. *Mol Neurobiol* 2008, **37**:83–90.

57. Magni G, Ceruti S: P2Y purinergic receptors: New targets for analgesic and antimigraine drugs. *Biochem Pharmacol* 2013, **85**:466–477.

58. Shimizu T: TRPV1 receptor as a therapeutical target for the treatment of migraine. *Brain Nerve* 2009, **61**:949–956.

59. Zimmermann M: Ethical guidelines for investigations of experimental pain in conscious animals. *Pain* 1983, **16**:109–110.

60. Park CK, Bae JH, Kim HY, Jo HJ, Kim YH, Jung SJ, Kim JS, Oh SB: Substance P sensitizes P2X3 in nociceptive trigeminal neurons. *J Dent Res* 2010, **89**:1154–1159.